Chaotic Modeling and Simulation (CMSIM) 2: 219–230, 2016

Synchronization of chaotic Cellular Neural Networks in small-world topology

Soriano-Sánchez A.G.[1], Platas-Garza M.A.[1], López-Gutiérrez R.M.[2], Cruz-Hernández C.[3], and Posadas-Castillo C.[1]

[1] Universidad Autónoma de Nuevo León - Facultad de Ingeniería Mecánica y Eléctrica (FIME-UANL).
Av. Pedro de Alba, S.N., Cd. Universitaria, C.P. 66451, San Nicolás de los Garza, N.L., México. (allansori@gmail.com, miguel.platasg@uanl.mx, cornelio.posadascs@uanl.edu.mx)

[2] Engineering Faculty, Baja California Autonomous University (UABC)
Carretera Ensenada-Tijuana Km. 103, C.P. 22860, Ensenada, B.C., México. (roslopez@uabc.edu.mx)

[3] Electronics and Telecommunications Department (CICESE)
Carretera Ensenada-Tijuana No. 3918, Zona Playitas, C.P. 22860, Ensenada, B.C., México. (ccruz@cicese.mx)

Abstract. In this paper by using chaotic Cellular Neural Networks (CNNs), authors investigate the synchronization of a complex network that displays the small-world property. We consider two different models of chaotic CNNs to compose the complex network. Newman-Watts algorithm is used to generate the long-range connections in an arrangement of N-coupled chaotic CNNs, which will allow a faster communication between the CNNs of the whole network. Authors will show how the small-world property allows us to synchronize a complex network by using a small coupling strength. Chaotic synchronization is achieved by using the complex systems theory. Numerical simulations are provided to show the effectiveness of this method.

Keywords: Synchronization, Complex network, Small-world property, Chaotic Cellular Neural Networks (CNNs).

1 Introduction

The so-called Cellular Neural Networks have been extensively studied since their beginning three decades ago. The main interest on this systems was and still is their ability for information or signal processing. The best features of these systems are: on one hand, their ability of real-time signal processing; on the other hand, their local interconnection makes them tailor-made for monolithic implementation [1,2]. The acronym CNN for Cellular Neural Network

Received: 20 March 2015 / Accepted: 14 December 2015

ISSN 2241-0503

was first introduced by L.O. Chua and L. Yang in 1988 [1]. Since its invention, many applications for CNNs have been proposed in literature [1–8], with special interest for image-processing tasks [9].

We are interested in the application that interpreted CNN as Cellular Nonlinear Networks. This interpretation was a extension of the original paradigm of CNN [2] proposed by Chua and Roska [10] in 1993. In this way, CNNs were considered for generating chaotic and hyper-chaotic signals [2,11–13], autowaves, spiral waves and spatial-temporal chaos [14,15]. In this work, we are interested in two different CNN that exhibit chaotic behavior, they will be briefly explained later on.

In addition to the complexity generated by locally coupled nonlinear dynamical systems to generate a specific behavior (in this case chaotic), we arrange the resulting CNN in certain way to generate a small-world network to be synchronize. Synchronization of complex networks has also been widely studied; nowadays the two most important results derived from this intense research are the following: firstly, the discovery that the behavior of biological and non-biological systems can be modeled by the dynamics of complex networks: modeling of economic systems [16], modeling of a community for engineering purposes [17,18], the spread of epidemics in a population [19,20] and modeling of the human brain [21]. Secondly, the influence or effect of topology on the realization of system processes: spreading of rumors [22], generation of memory capacity in a system [23] and fast transmission of information between individuals [23,24] for instance. The previously mentioned papers show results of complex networks arranged in small-world topology.

The small-world networks have their beginning in the 1960's. Stanley Milgram distributed letters to people in Nebraska to be sent to Boston by people who might know the consignee. Milgram found that it had taken an average of six steps for a letter to get from Nebraska to Boston [25,26]. The performed experiment led to the well-known concept of six degrees of separation [27]. Such networks became very popular after D.J. Watts and S.H. Strogatz published the pioneering algorithm to introduce the small-world property to a regular network. They showed that the network main characteristics were: high clustering coefficient and short average path length [26].

This paper is organized as follows: In Section 2 a brief review on complex networks and their synchronization is given. We also explain the Newman-Watts small-world algorithm in this section. The models of the chaotic Cellular Neural Networks (CNNs) which will be used as chaos generators are given in Section 3. Synchronization of N-coupled chaotic CNNs is provided in Section 4. Some conclusions are given in Section 5.

2 Complex networks

In the present paper we will use the definition of a complex network as suggested by Wang [28].

Definition 1 *A complex network is defined as an interconnected set of oscillators (two or more), where each oscillator is a fundamental unit, with its dynamic depending of the nature of the network.*

Each oscillator is defined as follows

$$\dot{\mathbf{x}}_i = f(\mathbf{x}_i) + \mathbf{u}_i, \qquad \mathbf{x}_i(0), \qquad i = 1,\ 2, \ldots,\ N, \tag{1}$$

where N is the network's size, $\mathbf{x}_i = [x_{i1},\ x_{i2},\ \ldots,\ x_{in}] \in \Re^n$ represents the state variables of the oscillator i. $\mathbf{x}_i(0) \in \Re^n$ are the initial conditions for oscillator i. $\mathbf{u}_i \in \Re^n$ establishes the synchronization between two or more oscillators and is defined as follows [29]

$$\mathbf{u}_i = c\sum_{j=1}^{N} a_{ij}\mathbf{\Gamma}\mathbf{x}_j, \qquad i = 1,\ 2, \ldots,\ N. \tag{2}$$

The constant $c > 0$ represents the coupling strength. $\mathbf{\Gamma} \in \Re^{n\times n}$ is a constant matrix to determine the coupled state variable of each oscillator. Assume that $\mathbf{\Gamma} = \text{diag}(r_1,\ r_2, \ldots,\ r_n)$ is a diagonal matrix. If two oscillators are linked through their k-th state variables, then, the diagonal element $r_k = 1$ for a particular k and $r_j = 0$ for $j \neq k$.

The matrix $\mathbf{A} \in \Re^{N\times N}$ with elements a_{ij} is the coupling matrix which shows the connections between oscillators, if the oscillator i-th is connected to the oscillator j-th, then $a_{ij} = 1$, otherwise $a_{ij} = 0$ for $i \neq j$. The diagonal elements of $\mathbf{A}$ matrix are defined as

$$a_{ii} = -\sum_{j=1, j\neq i}^{N} a_{ij} = -\sum_{j=1, j\neq i}^{N} a_{ji} \qquad i = 1, 2, ..., N. \tag{3}$$

The dynamical complex network (1) and (2) is said to achieve synchronization if

$$\mathbf{x}_1(t) = \mathbf{x}_2(t) = \ldots = \mathbf{x}_N(t) \ \text{ as } \ t \to \infty. \tag{4}$$

In this paper networks with N chaotic CNNs as nodes are considered to be synchronized.

2.1 Newman-Watts small-world algorithm

After Watts and Strogatz published their pioneering algorithm to generate small-world networks in 1998, a revised version of that algorithm emerged one year later. In 1999, M.E.J. Newman and D.J. Watts proposed a modified version of the original small-world model [30,31]. Newman-Watts algorithm also starts from the nearest-neighbor topology, which is a ring lattice with periodic boundary conditions. The algorithm introduces the small-world property by adding links to pairs of CNN randomly chosen. Restrictions are: a CNN cannot have multiple links with another CNN or a link with itself. In Fig. 1 an example of a small-world network created with this model is shown. Here, as mentioned before N is the network's size, k is the periodic boundary condition of the

nearest neighbor topology, the i-th CNN is connected with $i \pm 1, i \pm 2, \ldots, i \pm k$; p is the probability to add a link and $N(N-(2k+1))p/2$ are the number of long-range link.

The characteristics most affected by the small-world property will be: *the clustering coefficient* C, which is defined as $C_i = 2E_i/k_i(k_i-1)$, where E_i are the actual edges that exist between k_i CNNs of the total possible number $k_i(k_i-1)/2$; *the average path length* L, which is defined as the distance between two oscillators averaged over all pairs of oscillators [28]. Due to the existence of long-range links, the small-world network has high clustering coefficient $C(p)$, and a short average path length $L(p)$.

In this paper we will use the Newman-Watts algorithm because as revised version of the original Watts-Strogatz algorithm, it prevents from the generation of isolated clusters.

3 Cellular Neural Networks (CNNs) models

In this section the models of chaotic Cellular Neural Networks (CNNs) will be presented and briefly described.

First of all, authors resort to the following definition of a Cellular Neural Network (CNN) [1].

Definition 2 *A standard CNN architecture consists of an $M \times N$ rectangular array of cells. Each cell is a dynamical system which has an input and a state evolving according to some prescribed dynamical laws. Each cell is coupled only among the neighboring cells lying within some prescribed sphere of influence with radius r, i.e., the r-neighborhood of the cell. The cell in row i and column j is denoted as $C(i,j)$ and it is said to be isolated if it is not coupled to any other cell.*

The variables for an isolated cell are [1]: input $u(t) \in \Re^u$, threshold $z(t) \in \Re^z$, state $x(t) \in \Re^x$ and output $y(t) \in \Re^y$. An example of an isolated cell is given in Fig. 2. For this particular case, we used the following models.

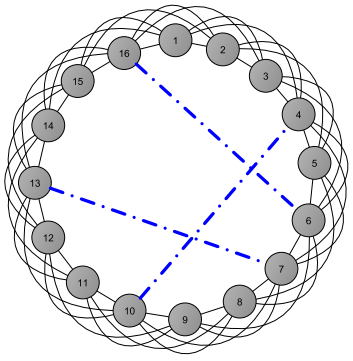

Fig. 1. Small-world network created adding some links between randomly chosen pair of chaotic CNNs. The solid lines are all the existing links. The dash-dot lines are the links randomly added.

3.1 Chaotic 3D CNN model

The chaotic 3D CNN [32] is described by the following equation

$$\dot{\mathbf{x}} = -\mathbf{x} + \mathbf{T}\tanh(\mathbf{x}), \tag{5}$$

where the state vector $\mathbf{x} \in \Re^3$, $\tanh(\mathbf{x}) = [\tanh(x_1)\ \tanh(x_2)\ \tanh(x_3)]^T$ and

$$\mathbf{T} = \begin{bmatrix} T_{11} & T_{12} & T_{13} \\ T_{21} & T_{22} & T_{23} \\ T_{31} & T_{32} & T_{33} \end{bmatrix} = \begin{bmatrix} 1.49 & 2 & 1 \\ -2 & 1.7 & 0 \\ 4 & -4 & 2 \end{bmatrix}. \tag{6}$$

The 3D CNN described in Eqn. (5) exhibits chaotic behavior for parameters given in Eqn. (6) [32]. An example of the chaotic attractor and state variables are shown in Fig. 3 (a) and Fig. 3 (b) respectively. They were obtained by using the initial conditions $\mathbf{x}(0) = [-0.2,\ 0.1,\ 0.1]^T$.

3.2 Standard CNN model

In this work, we also consider the standard CNN model proposed in [1], which is widely used for $M \times N$ arrays. The standard CNN equations are the following

$$\dot{x}_{ij} = -x_{ij} + z_{ij} + \sum_{kl \in N_r(i,j)} a_{kl} y_{kl} + \sum_{kl \in N_r(i,j)} b_{kl} v_{kl}, \quad i = 1, \ldots, M; j = 1, \ldots, N, \tag{7}$$

$$y_{ij} = f(x_{ij}), \tag{8}$$

where z_{ij} is a scalar for simplicity, $N_r(i,j)$ is the sphere of influence with radius r, i.e., the r-neighborhood of the cell. $\sum_{kl \in N_r(i,j)} a_{kl} y_{kl}$ and $\sum_{kl \in N_r(i,j)} b_{kl} v_{kl}$ are the local couplings, and

$$f(x_{ij}) = \frac{1}{2}\left(|x_{ij} + 1| - |x_{ij} - 1|\right). \tag{9}$$

For the particular case where $M = 3$ and $N = 4$, the Eqns. (7)-(8) assume the simpler form of a 3×4 CNN array [1]

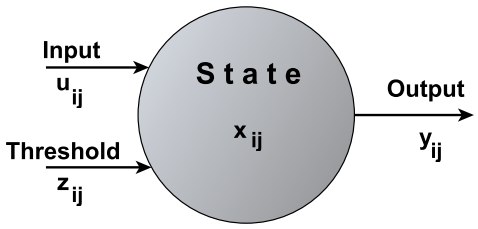

Fig. 2. A two-dimensional isolated cell: input $u_{ij}(t) \in \Re^u$, threshold $z_{ij}(t) \in \Re^z$, state $x_{ij}(t) \in \Re^x$ and output $y_{ij}(t) \in \Re^y$

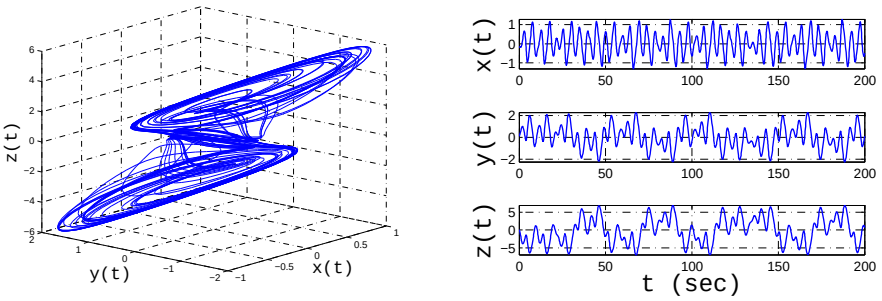

(a) (b)

Fig. 3. (a) View $x - y - z$ for the chaotic attractor of the 3D CNN in Eqn. (5). (b) $x(t)$, $y(t)$ and $z(t)$ states variables obtained with $\mathbf{x}(0) = [-0.2,\ 0.1,\ 0.1]^T$.

$$\begin{cases} \dot{x}_1 = -x_1 + a_{00}f(x_1) + a_{01}f(x_2) + b_{00}v_1(t), \\ \dot{x}_2 = -x_2 + a_{0,-1}f(x_1) + a_{00}f(x_2) + b_{00}v_2(t), \\ y_1 = f(x_1), \\ y_2 = f(x_2), \end{cases} \tag{10}$$

where $a_{00} = 2$, $a_{0,-1} = 1.2$, $a_{01} = -1.2$, $b_{00} = 1$, $v_1(t) = 4.04sin\left(\frac{\pi}{2}t\right)$ and $v_2(t) = 0$; then the set of equations (10) becomes

$$\begin{cases} \dot{x}_1 = -x_1 + 2f(x_1) - 1.2f(x_2) + 4.04sin\left(\frac{\pi}{2}t\right), \\ \dot{x}_2 = -x_2 + 1.2f(x_1) + 2f(x_2), \end{cases} \tag{11}$$

with the nonlinear function

$$f(x_{1,2}) = \frac{1}{2}\left(|x_{1,2} + 1| - |x_{1,2} - 1|\right). \tag{12}$$

Fig. 4 (a) and Fig. 4 (b) show an example of the chaotic attractor and the state variables respectively generated with Eqns. (11)-(12).

In the remainder of the paper, complex networks with small-world topology composed by the previously described CNN models will be synchronized.

4 Synchronization of N chaotic CNNs via coupling matrix

In this section, synchronization of complex networks composed of N-coupled chaotic CNNs is achieved. Firstly, necessary conditions to achieve synchronization are provided. Then, at the end of the section synchronization results are shown.

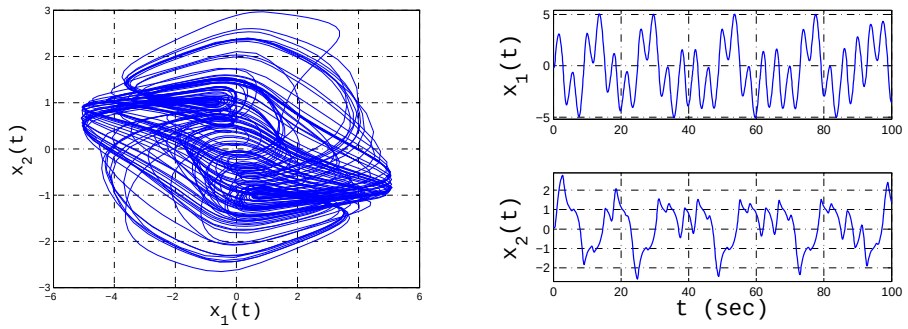

(a) (b)

Fig. 4. (a) View $x_1 - x_2$ for the chaotic attractor of the standard CNN in Eqn. (11)-(12). (b) $x_1(t)$ and $x_2(t)$ state variables obtained with $\mathbf{x}(0) = [-0.2,\ 0.1]^T$.

4.1 Conditions for synchronization by using the coupling matrix

Suppose that there are no isolated clusters in the network, then the coupling matrix $\mathbf{A}$, obtained as explained in Section 2, is a symmetric irreducible matrix, so one eigenvalue of $\mathbf{A}$ is zero and all the other eigenvalues are strictly negative, this means, $\lambda_{2,\ldots,N}(A) < 0$.

Theorem 1 ([28]) *Consider the dynamical network (1). Let*

$$0 = \lambda_1 > \lambda_2 \geq \lambda_3 \cdots \geq \lambda_N, \tag{13}$$

be the eigenvalues of its coupling matrix $\mathbf{A}$*. Suppose that there exist an* $n \times n$ *diagonal matrix* $\mathbf{D} > 0$ *and two constants* $\bar{d} < 0$ *and* $\tau > 0$*, such that*

$$[Df\,(s\,(t)) + d\Gamma]^T\,\boldsymbol{D} + \boldsymbol{D}\,[Df\,(s\,(t)) + d\Gamma] \leq -\tau \boldsymbol{I}_n, \tag{14}$$

for all $d \leq \bar{d}$*, where* $\boldsymbol{I}_n \in \Re^{n\times n}$ *is an unit matrix. If moreover,*

$$c\lambda_2 \leq \bar{d}, \tag{15}$$

then the synchronization state (4) is exponentially stable.

The coupling strength c determines the stability of the synchronization state (Eqn. (4)) through the control law (Eqn. (2)). It is obtained as follows

$$c \geq \left| \frac{\bar{d}}{\lambda_2} \right|. \tag{16}$$

4.2 Synchronization results

In this section two complex networks of identical chaotic Cellular Neural Networks will be synchronized. The original topology of the network is similar to

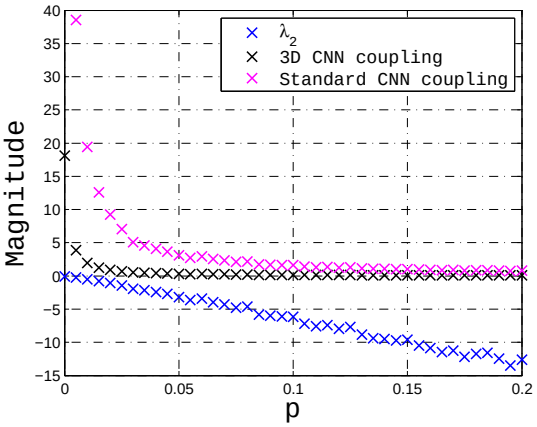

Fig. 5. Lowest boundaries of c corresponding to $\lambda_2(p)$ for a complex network composed of $N = 100$ CNN with a periodic boundary condition $k = 3$.

the one illustrated in Fig. 1 with $N = 100$ and a periodic boundary condition $k = 3$. The long-range connections will be added as p grows according to the Newman-Watts small-world algorithm. Every node in the network will be either a chaotic 3D CNN described by Eqns. (5)-(6) or a chaotic standard CNN described by Eqns. (11)-(12).

Considering a synchronization scheme of N-coupled chaotic CNN, the coupling matrix is obtained as explained in Section 2. All its eigenvalues are $0 = \lambda_1 > \lambda_2 \geq \lambda_3 \ldots \geq \lambda_{100}$. For Case 1 and Case 2, initial conditions were randomly generated for each oscillator within the range $[-5, 5]$ without repeating them. The Gamma matrix is defined as $\Gamma = \mathrm{diag}(1, 0, 0)$ also for both cases. This means that the synchronization is achieved by the first state variable. According to Eqn. (2), the control laws u_{i1} for $i = 1, \ldots, 100$ are given by the A matrix nonzero elements.

For the computation of the coupling strength, we will use the data depicted in Fig. 5. Firstly, we provide the second largest eigenvalue ("x"-mark in blue) as a function of the probability p. Secondly, for each λ_2, we computed the coupling strength c value according to Eqn. (16). The obtained ratio is the lowest boundary necessary for each type of CNN to reach synchrony and it decreases as the probability increases.

Case 1: Synchronization of N chaotic 3D CNN By using $\bar{d} = -1$ we stabilize the states of a single chaotic 3D CNN. Now, we compute from Eqn. (16) that $c \geq |-1/\lambda_2|$. Note that we have only to determine λ_2, which will vary as the network varies through the probability p. In Fig. 5 the coupling strength lowest boundary corresponding to each λ_2 is given with "x"-mark in black.

The equations that describe the complex network are given as follows

$$\dot{\mathbf{x}}_i = -\mathbf{x}_i + \mathbf{T}\tanh(\mathbf{x}_i) + \mathbf{u}_i, \qquad i = 1, \ldots, 100, \tag{17}$$

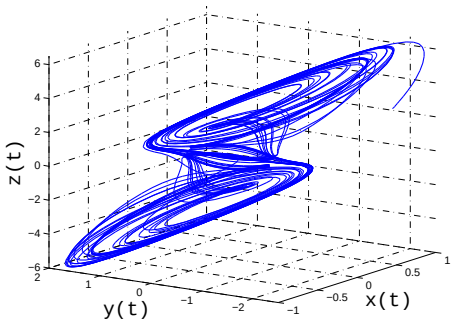

Fig. 6. View $x - y - z$ for the chaotic attractor of the 3D CNN of Eqns. (17)-(18).

and

$$\mathbf{T} = \begin{bmatrix} T_{11} & T_{12} & T_{13} \\ T_{21} & T_{22} & T_{23} \\ T_{31} & T_{32} & T_{33} \end{bmatrix} = \begin{bmatrix} 1.49 & 2 & 1 \\ -2 & 1.7 & 0 \\ 4 & -4 & 2 \end{bmatrix}. \tag{18}$$

For this case by using $p = 0.15$ and coupling strength at $c = 1$, the following synchronization results were obtained: In Fig. 6 the chaotic attractor of the final dynamic of Eqns. (17)-(18) is shown. In Fig. 7 (a) the time evolution of the state variables is shown. Fig. 7 (b) provides the phase portraits between some state variables to verify synchronization, here the condition $\mathbf{x}_1(t) = \mathbf{x}_2(t) = \ldots = \mathbf{x}_N(t)$ as $t \to \infty$ holds.

Case 2: Synchronization of N standard CNN By using $\bar{d} = -10$ the two state variables $x_1(t)$ and $x_2(t)$ of a single standard CNN are stabilized. The same way that in the previous case, we compute from Eqn. (16) the coupling

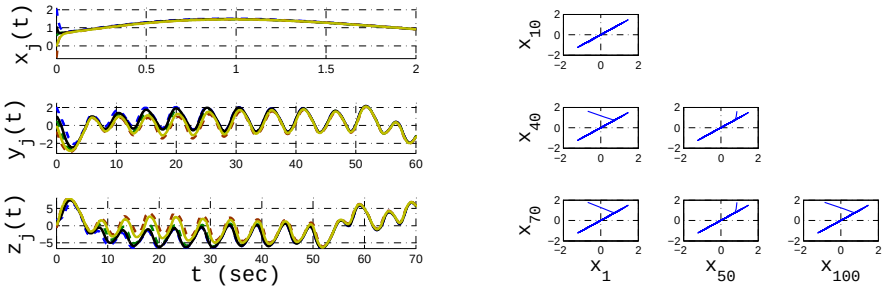

(a) (b)

Fig. 7. (a) State variables $x_j(t)$, $y_j(t)$ and $z_j(t)$ for $j = 24,\ 49,\ 53,\ 63,\ 68$ randomly chosen. (b) Phase portrait between x_i vs. x_j; $i = 1,\ 50,\ 100$; $j = 10,\ 40,\ 70$ state variables.

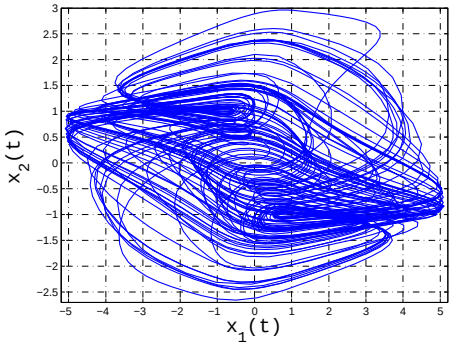

Fig. 8. View $x_1 - x_2$ for the chaotic attractor of the standard CNN of Eqns. (19)-(20).

strength. In Fig. 5 the coupling strength lowest boundary corresponding to each λ_2 is given for this case with "x"-mark in magenta.

The equations that describe the complex network are given as follows

$$\begin{cases} \dot{x}_{i1} = -x_{i1} + 2f(x_{i1}) - 1.2f(x_{i2}) + 4.04sin\left(\frac{\pi}{2}t\right) + u_{i1}, \\ \dot{x}_{i2} = -x_{i2} + 1.2f(x_{i1}) + 2f(x_{i2}), \qquad i = 1, \ldots, \ 100, \end{cases} \tag{19}$$

with the nonlinear function

$$f(x_{i1,2}) = \frac{1}{2}\left(|x_{i1,2} + 1| - |x_{i1,2} - 1|\right). \tag{20}$$

For this case by using $p = 0.8$ and coupling strength at $c = 0.5$, the following synchronization results were obtained: In Fig. 8 the chaotic attractor of the final dynamic of Eqns. (19)-(20) is shown. The time evolution of some state variables randomly chosen is shown in Fig. 9 (a). In Fig. 9 (b) synchronization can

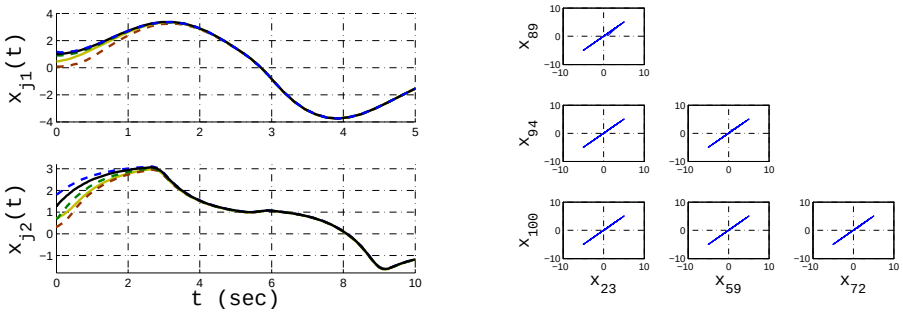

(a) (b)

Fig. 9. (a) State variables $x_{j1}(t)$ and $x_{j2}(t)$ for $j = 23,\ 59,\ 72,\ 89,\ 100$ randomly chosen. (b) Phase portrait between x_i vs. x_j; $i = 23,\ 59,\ 72$; $j = 89,\ 94,\ 100$ state variables.

be verified by the phase portraits between some state variables. As in the previous case, the synchronization condition $\mathbf{x}_1(t) = \mathbf{x}_2(t) = \ldots = \mathbf{x}_N(t)$ as $t \to \infty$ holds.

We highlight the fact that synchronization of complex networks of chaotic CNN was achieved by using a small coupling strength c in small-world topology.

5 Conclusion

In this work the synchronization of small-world networks composed by chaotic Cellular Neural Networks (CNNs) was achieved. We highlight that it was possible to synchronize chaotic CNN arrays disposed in a small-world topology by using the Complex Systems Theory. A remarkable thing in this paper is the fact that the complex networks under consideration, either composed by the 3D CNN or the standard CNN, can achieve synchrony by using a small coupling strength c. Numerical simulations showed that the bigger the probability p, the easier to synchronize the complex network.

6 Acknowledgment

This work was supported by CONACYT México No. 166654, PAICYT IT956-11 and Facultad de Ingeniería Mecánica y Eléctrica (FIME-UANL).

References

1. L.O. Chua and L. Yang, *Cellular Neural Networks: Theory and applications*, IEEE Trans. Circuits Syst. **35**, pp. 1257-1290, 1998.
2. Müstak E. Yalçin, Johan A. K. Suykens, Joos P.L. Vandewalle, *Cellular Neural Networks, Multi-Scroll Chaos and Synchronization.*
3. A.R. Trivedi, S. Datta and S. Mukhopadhyay. *Application of Silicon-Germanium Source Tunnel-FET to Enable Ultralow Power Cellular Neural Network-Based Associative Memory*, IEEE Trans. Elect. Devices **61**(11), pp. 3707-3715, 2014.
4. B. Zineddin, Z. Wang and Xiaohui Liu. *Cellular Neural Networks, the NavierStokes Equation, and Microarray Image Reconstruction*, IEEE Trans. Image Processing **20**(11), pp. 3296-3301, 2011.
5. M. Di Federico, P.S. Mandolesi, P. Julián and A.G. Andreou. *Experimental results of simplicial CNN digital pixel processor*, Electronic Letters **44**(1), 2008.
6. E. Cesur, N Yildiz and V. Tavsanoglu. *On an Improved FPGA Implementation of CNN-Based Gabor-Type Filters*, IEEE Trans. Circuits and Systems-II: Express Briefs **59**(11), pp. 815-819, 2012.
7. M. Di Federico, P. Julián and P.S. Mandolesi. *SCDVP: A Simplicial CNN Digital Visual Processor*, IEEE Trans. Circuits and Systems-I: Regular Papers **61**(7), pp. 1962-1969, 2014.
8. H. Serrano-Guerrero, C. Cruz-Hernández, R.M. López-Gutiérrez, C. Posadas-Castillo and E. Inzunza-González. *Chaotic Synchronization in Star Coupled Networks of Three- Dimensional Cellular Neural Networks and Its Application in Communications*, Int. J. Nonlinear Sci. Numer. Simul. **11**(8), pp. 571580, 2011.
9. L.O. Chua and T. Roska. *Cellular neural networks and visual computing*, Fundations and applications, Cambridge University, 2001.

10. L.O. Chua and T. Roska. *The CNN paradigm*, IEEE Trans. Circuits and Systems-I **40**(3), pp.147-156, 1993.
11. J.A. Suykens and L.O. Chua. *n-double scroll hypercubes in 1D-CNNs*, Int. J. Bifurcation and Chaos **7**(8), pp. 1873-1885, 1997.
12. I. Petras, T. Roska and L.O. Chua. *New spatial-temporal patterns and the first programmable on-chip bifurcation test bed*, IEEE Trans. Circuits and Systems-I **50**(5), pp. 619-633, 2003.
13. T. Kapitaniak, L.O. Chua and G.Q. Zhong. *Experimental hyperchaos in coupled Chua's circuits*, IEEE Trans. Circuits and Systems-I **41**(7), pp. 499-403, 1994.
14. L.O. Chua. *CNN: a paradigm for complexity*, World Scientific, Singapore, 1998.
15. L.O. Chua, M. Hasler, G.S. Moschytz and J. Neirynck. *Autonomous cellular neural networks: a unified paradigm for pattern formation and active wave propagation*, IEEE Trans. Circuits and Systems-I **42**(10), pp. 559-577, 1995.
16. V. Latora, M. Marchiori. *Economic small-world behavior in weighted networks*, Eur. Phys. J. B **31**, pp. 249-263, 2003.
17. A.G. Soriano-Sánchez, C. Posadas-Castillo, M.A. Platas-Garza and D.A. Diaz-Romero. *Performance improvement of chaotic encryption via energy and frequency location criteria*, Math. Comput. Simul. **doi**:10.1016/j.matcom.2015.01.007, 2015.
18. A. Soriano-Sánchez, C. Posadas-Castillo, M.A. Platas-Garza, R.M. López-Gutiérrez and C. Cruz-Hernández. *Chaotic synchronization of irregular complex networks with multi-scroll attractors Genesio & Tesi 3-D*, Proceedings of the 2013 International Conference on Systems, Control and Informatics pp. 237-243, Venice, Italy.
19. F. C. Santos, J. F. Rodrigues, J. M. Pacheco. *Epidemic spreading and cooperation dynamics on homogeneous small-world networks*, Physical Review E **72** 056128, 2005.
20. Z. Wang, H. Zhang, Z. Wang. *Multiple effects of self-protection on the spreading of epidemics*, Chaos, Solitons and Fractals **61**, pp. 1-7, 2014.
21. Olaf Sporns. *The human connectome: a complex network*, Ann. N.Y. Acad. Sci. **1224**, pp. 109-125, 2011.
22. D. H. Zanette. *Dynamics of rumor propagation on small-world networks*, Physical Review E **65** 041908.
23. N. Davey, B. Christianson, R. Adam. *High Capacity Associative Memories and Small World Networks*, Neural Networks 2004, Proceedings IEEE International Joint Conference.
24. L. Guzmán-Vargas, R. Hernández-Pérez. *Small-world topology and memory effects on decision time in opinion dynamics*, Physica A **372**, pp. 326-332, 2006.
25. S. Milgram. *The Small-World Problem*, Psychology Today **1**(1), pp. 61-67, 1967.
26. D. J. Watts and S. H. Strogatz. *Collective dynamics of "small-world" networks*, Nature **393**, pp. 440-442, 1998.
27. J. Guare. *Six Degrees of Separation: A Play*, Vintage, New York, 1990.
28. Xiao Fan Wang. *Complex Networks: Topology, Dynamics and Synchronization*, Int. J. of Bifurcation and Chaos, Vol. 12, No. 5 (2002) 885-916.
29. Xiao Fan Wang and Guanrong Chen. *Synchronization in small-world dynamical networks*, Int. J. of Bifurcation and Chaos, Vol. 12, No. 1 (2002) pp. 187-192.
30. M.E.J. Newman and D.J. Watts. *Renormalization group analysis of the small-world network model*, Phys. Lett. A **263**, pp. 341-346, 1999a.
31. M.E.J. Newman and D.J. Watts. *Scaling and percolation in the small-world network model*, Phys. Rev. E **60**, pp. 7332-7342, 1999b.
32. X.S. Yang and Q. Li. *Horseshoe chaos in cellular neural networks*, International Journal of Bifurcation and Chaos, **16**, pp. 157-161, 2006.